

---

# Oscillator Purity Fundamentals

## 2

---

---

### ***1 Introduction***

A sinusoidal oscillation is described completely by its amplitude and frequency. The purity of the oscillation pertains typically to only the frequency or period of oscillation. This is because an oscillator is typically used to synchronize events in time. This applies to wireless transceivers as well as digital circuits. The amplitude of oscillation, once above a threshold value, is typically irrelevant as long as it can generate an action (event) on the subsequent circuit block. An oscillation that is perfectly pure has a constant period of repetition. In frequency domain, the perfect repetition translates into a single tone, for a sinusoidal oscillation anyway.

Historically, observing periodicity in time predates the observation of spectral purity for obvious reasons. Ancient Egyptians noted that Sirius rises to its place besides the sun exactly every 365 days. They divided the year into twelve 30-day months and a short 5 day month that was called the “little month”. Their calendar is still used today by peasants in the countryside of Egypt, side-by-side with the Gregorian calendar, as it fits perfectly the Egyptian climate and the flooding of the Nile. Their calendar was the basis of the modern calendar we use today. The Babylonians of today’s Iraq used a lunar calendar that follows the periodicity of the moon, a cycle of 29 to 30 days. They are the ones who divided the day into smaller units that relate to their base-60 numeral system. Around the 16<sup>th</sup> century, in the era of great expeditions, there was a great need for accurate clocks for navigation. Determining longitude accurately was not possible without a tool that can tell time with

great accuracy [1]. Galileo sketched out the concept of the first pendulum-based clock. It was Harrison who first implemented a clock that can tell time within one second of error per day [1]. Various designs of mechanical movements were implemented over the centuries that followed and are perfected today in Swiss mechanical watches. The 1920s witnessed the first quartz clock that enabled much higher frequency/period stability. Later, this fueled the clock industry in Japan. For more accurate time bases, the atomic clock is used as a calibration source. The search for the most accurate clock is in essence the search for a high long-term stability signal source. The question of noise in signal sources was not of concern until World War II. Only then was the study of noise in the oscillator's phase born. In essence, phase noise relates to the short-term stability of the oscillator's period, frequency, or phase.

Signal purity measures can be divided into two main categories: deterministic and stochastic. Deterministic *impurity* comes from spurious signals that show in the signal spectrum as delta-Dirac impulses, known as *spurs* at a fixed frequency offset from the main tone. Stochastic *impurity* arises from stochastic variation of signal phase and are manifested in noise skirts around the fundamental frequency. Another way of quantifying stochastic purity is by looking at the signal in time domain where stochastic perturbations are manifested as perturbations in the zero crossings of the sinusoidal waveform. For practical RF receiver design purposes, amplitude perturbations are typically of little concern because mixers are not sensitive to them. In transmitters, however, the situation is somewhat different. Amplitude noise would interfere with neighboring channels just as phase or frequency noise does if it spills out of its allotted bandwidth.

In this chapter we briefly describe the basic concepts of signal purity both in time and frequency domains. The reader who is familiar with these concepts can skip this chapter and advance to chapter 3.

---

## 2 Timing Jitter

A pure oscillation repeats in time precisely every  $T$  seconds, where  $T$  is called the oscillation *period*. In other words, if we set a particular threshold voltage level, the oscillation waveform will cross this threshold in a given direction precisely every  $T$  seconds. In the presence of noise, the points in time where

the oscillation waveform crosses this threshold are dithered around their ideal noiseless locations. In statistical terms, the oscillation waveform is a random process described by:

$$V(\phi_n, t) = A \sin(\omega_o t + \phi_n), \quad (1)$$

where  $\phi_n$  is a stochastic process that produces a random phase fluctuation.

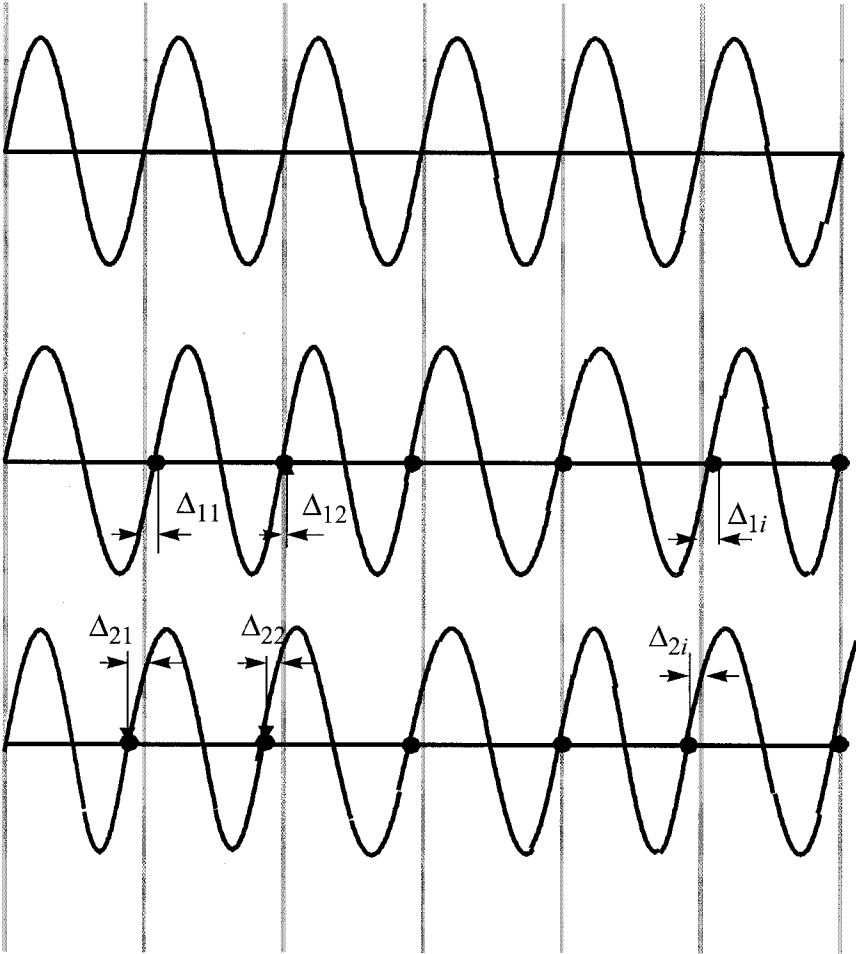
Consider now different realizations of this random process, i.e. different possible waveforms that fulfill (1). Such realizations are shown in Figure 1. The first waveform is an ideal noiseless oscillation. The other two waveforms are sample realizations for different values of  $\phi_n(t)$  that have the same statistical properties. The threshold is held at the  $V(t) = 0$ . As shown, each of the two realizations rises through the threshold at random time points around the ideal waveform crossing points. The difference in the crossing time between the ideal waveform and the various realizations is a random process denoted by  $\Delta_{ji}$ . It is assumed that all of the realizations of the random process  $V(\phi_n, t)$  start from the same zero initial phase. The subscript  $j$  denoted the realization number whereas the subscript  $i$  denotes the count of the threshold crossing starting from the initial phase at  $i = 0$ .

At any particular zero crossing  $i$ , the difference in crossing times is a random variable that has some particular mean and variance. Consider the zero<sup>th</sup> crossing, i.e. at the initial point; all values of  $\Delta_{j0}$  are equal to zero because all realizations of  $V(\theta, t)$  start at the same initial phase. Therefore, the random variable  $\Delta_{j0}$  has zero mean and zero variance. In other words, the probability distribution of  $\Delta_{j0}$  is an impulse,

$$\langle \Delta_{j0} \rangle = 0, \langle \Delta_{j0}^2 \rangle = 0, P(\Delta_{j0}) = \delta(\Delta), \quad (2)$$

where  $\delta$  is the delta-Dirac impulse.

Now comes into play, the most characteristic property of oscillators; they are autonomous circuits. The phase of the oscillator is determined only from within. This means that the ending point of cycle 1 is the starting point of cycle 2 and the phase error incurred in cycle 1 is carried over without correction to cycles 2 and 3, .... indefinitely. This is manifested in the basic mathematical model of oscillators shown in Chapter 1; the oscillator is a phase integrator. This means that if we try to evaluate the statistical properties of  $\Delta$  at the end of cycle  $m$  ( $\Delta_{jm}$ ), we are actually looking at the accumulation (inte-

FIGURE 1 *Different realizations of a random phase jitter process.*

gration) of all  $\Delta_{ji}$  from  $i = 0$  to  $i = m$ . If we assume for any realization  $j = n$ , the random fluctuations causing phase jitter are due to white noise (uncorrelated from sample to sample), then the variance of  $\Delta_{ni}$  grows linearly with time. This was experimentally verified on ring oscillators in [2] but is true for all oscillators. What we have just described is often called absolute jitter [3]. It describes the accumulation of timing jitter with respect to an ideal noiseless

source. It was shown that the variance of the absolute jitter  $\Delta$  as given by McNeil (using his original notation) is:

$$\sigma_{\Delta}^2 = \kappa^2 t, \quad (3)$$

where  $\kappa$  is a time domain figure of merit of the oscillator. The higher the oscillator quality factor,  $Q$ , the lower the factor  $\kappa$ . The variable  $t$  is time or the measurement interval.

The resulting phase jitter from absolute jitter  $j$  is given by

$$\theta_n = 2\pi \frac{\Delta_n}{T}. \quad (4)$$

Note that  $\theta_n$  is evaluated only at the zero crossings, unlike the phase noise process discussed later, which is defined for all time. Timing jitter measures described here are useful in the world of digital circuits and optical communications clock recovery. Both application domains use square wave like signals and interface to circuits that operate only on the edges of the waveform. Therefore, it is rather common to describe the signal purity in the domains in terms of jitter in picoseconds. In the world of radio-frequency electronics, jitter is almost never used. This is because the signals are sine wave like and phase noise is more relevant as we will see later.

Herzel [4] rewrites (3) as

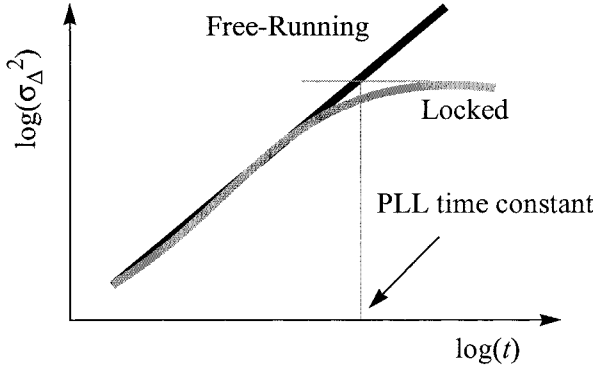
$$\sigma_{\theta}^2 = 2Dt, \quad (5)$$

where  $D$  is called the *diffusivity*. Ham calls  $D$ , the diffusion constant by analogy to the diffusion equation known as Einstein's relation, commonly used in solid-state physics to describe diffusion currents and applicable to any physical diffusion process [5]. This particular treatment is based on the seminal work of Melvin Lax in 1967 in which he analyzed noise in oscillators and showed that the oscillator spectrum (or linewidth) broadens in the presence of noise [6]. We will visit this result in the next subsection. Herzel also draws the same analogy in [7].

As shown by (3) and (5), absolute jitter in a free running oscillator grows indefinitely without bound. Note that we assume that noise in the oscillator is uncorrelated from one cycle to the next, which means that flicker noise is not

considered. Flicker noise is correlated from one sample to the next and represents deep system memory. To date, there is no mathematical treatment to describe absolute jitter in a free-running oscillator in the presence of flicker noise. It is also worth mentioning that if the oscillator is locked to a stable source in a phase-locked loop (PLL) absolute jitter does not grow indefinitely. Rather, it grows linearly until the measurement interval is within the loop time constant. In other words, the PLL cannot correct for fast jitter, but it does respond to jitter that is slower than the loop dynamics. This observation is shown in Figure 2 depicting, on a log-log scale, the absolute jitter versus time in a free-running and a locked oscillator.

FIGURE 2 Absolute jitter in locked and free-running oscillators.



Absolute jitter is not of much use in practice. Being unbounded, little use can be made out of it. A more important jitter measure is called cycle-to-cycle jitter [8] or period jitter [3]. In any oscillation period, this type of jitter is defined as the difference between the true instantaneous period of oscillation and the ideal (or long term average) period of oscillation. The name cycle-to-cycle jitter can be a little misleading and therefore we will use the name period jitter. It can be defined as

$$j_n \equiv t_{n+1} - t_n - T, \quad (6)$$

where  $t_{n+1}$  and  $t_n$  are the end and beginning time points of the  $n^{\text{th}}$  oscillation cycle [3].  $T$  is the period of noise-free oscillation. If we assume that the oscillation frequency is fixed (pure phase modulation) then  $T$  is also the average period of the noisy oscillation. Considering again thermal noise only, the jitter

in the  $n^{\text{th}}$  cycle is uncorrelated with the jitter all other cycles. In this case, it should be obvious that the absolute jitter variance given by (3) is merely the accumulation of  $\sigma_{jn}^2$  over all cycles from  $t = 0$  until  $t = nT$ . Therefore, (3) can be used to predict the RMS value of the period jitter using the substitution  $t = T$ , i.e. a measurement interval of one oscillation period,

$$\sigma_j^2 = \kappa^2 T. \quad (7)$$

---

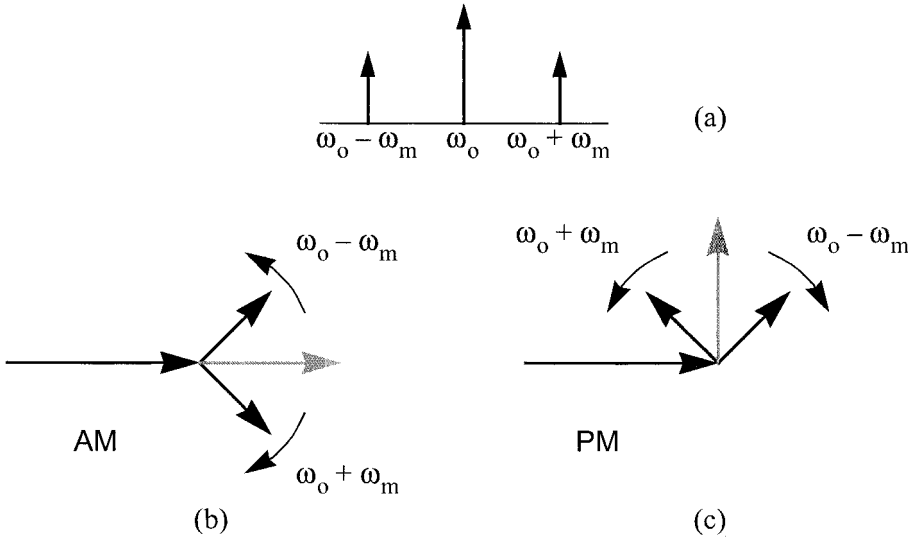
### 3 Recognizing Phase Noise

Consider a pair of sidebands around an oscillation frequency, as shown in Figure 3. Depending on the relative phase of these sidebands, one can have amplitude modulation or phase modulation. If, for instance, the sidebands sum together such that the sum is co-linear at all times with the carrier phasor, amplitude modulation results. On the other hand, if one of the sidebands is flipped, the sum is always orthogonal to the carrier, in which case phase modulation results. This idea will be used in the subsequent analysis.

---

FIGURE 3 *Sideband magnitude does not reveal modulation (a). Vector diagram shows that if sidebands sum co-linear to the carrier, AM (b); if orthogonal, PM (c).*

---



For example, if it is assumed the carrier is a cosine, the various modulation terms are easily derived and given in (8).

$$v_{\text{out}}(t) = V_1 \cos(\omega_o t) + \phi_1 (\cos(\omega_l t) - \cos(\omega_u t)) + \alpha_1 (\cos(\omega_l t) + \cos(\omega_u t)) + \phi_2 (\sin(\omega_l t) + \sin(\omega_u t)) + \alpha_2 (\sin(\omega_l t) - \sin(\omega_u t)), \quad (8)$$

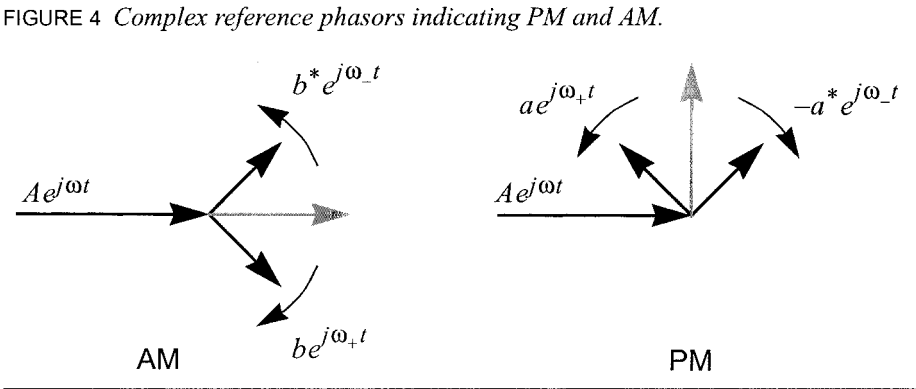
where the  $\phi_1$  and  $\phi_2$  terms are PM sidebands and  $\alpha_1$  and  $\alpha_2$  are AM sidebands.

It is easily seen how each pair contributes either only PM or AM sidebands by drawing a phasor diagram. For the  $\alpha_1$  term, both phasors are parallel to the carrier. Likewise the  $\phi_2$  pair are orthogonal. The other two cases are easily seen by allowing the phasors to rotate with time until they are either parallel or orthogonal with the carrier.

Working with all of these sine and cosine terms becomes difficult and distracting. A simpler notation can be used to capture the AM and PM components. In (9), the  $a$  sideband represents PM and the  $b$  sideband represents AM.

$$V_1 = Ae^{j\omega t} + (a_1 e^{j\omega_+ t} - a_1^* e^{j\omega_- t}) + (b_1 e^{j\omega_+ t} + b_1^* e^{j\omega_- t}) \quad (9)$$

Figure 4 illustrates these phasors in the complex domain.





---

## **4 Single Sideband Contains AM and PM**

A noise spectrum can be approximated by combining a large number of sinusoids whose frequencies are distributed over the range of interest and whose phase is random [16]. In particular, for this analysis, the noise is partitioned into bins of a particular bandwidth, say 1 Hz, and the noise in that bin is approximated by a single sinewave. The frequency of the sinewave is the center frequency of the bin, the amplitude is set such that it has the same power as the noise it represents, and the phase is random. This is a good approximation as long as you observe the noise for a time substantially less  $1/\Delta f$ , where  $\Delta f$  is the bin bandwidth. The reason is if you observe for longer periods, you can resolve the discrete tones in the approximation and so can distinguish the approximation from the original system.

Consider the case where the noise is combined with a large periodic carrier signal. If the noise is stationary and is added to the carrier, then the phases of each of the sinusoids that make up the approximation of the noise are uncorrelated. In this case, the noise is referred to as “additive noise”. Now consider only the noise at a fixed offset frequency  $\delta\omega$  from the carrier. As shown in Figure 5, this additive noise can be decomposed into equal amounts of amplitude and phase modulation. Both forms of modulation have components at  $\omega_+ = \delta\omega$  and  $\omega_- = -\delta\omega$ , but in this case the components combine to reinforce each other at  $\omega_+$  and cancel each other at  $\omega_-$ . Thus, additive noise consists of equal amounts of AM and PM noise.

A key observation of this work is that nonlinear circuits respond differently to AM and PM. For example, if an AM input is applied to a limiting amplifier, the output is clipped, removing the AM sidebands, Figure 6. Therefore, the circuit clips voltage or current. However, since it cannot clip along the time axis, PM signals are unaffected. For a PM signal to be unaffected means that the carrier-to-PM sideband ratio of the input is equal to the carrier-to-PM ratio of the output.

---

## **5 Phase Noise**

Phase noise is characterized using the phase perturbation spectral power in a 1 Hz bandwidth at some offset  $f_m$  from the center frequency normalized to the

FIGURE 5 Single noise component decomposed into AM and PM component.

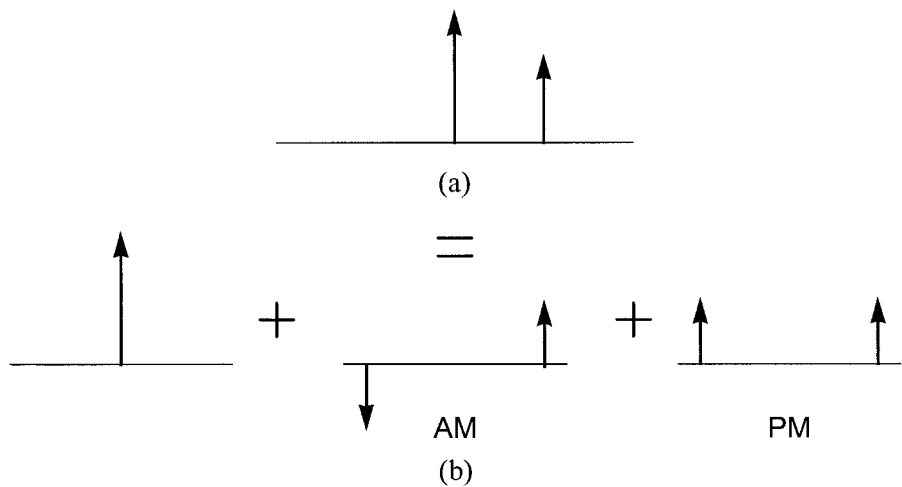
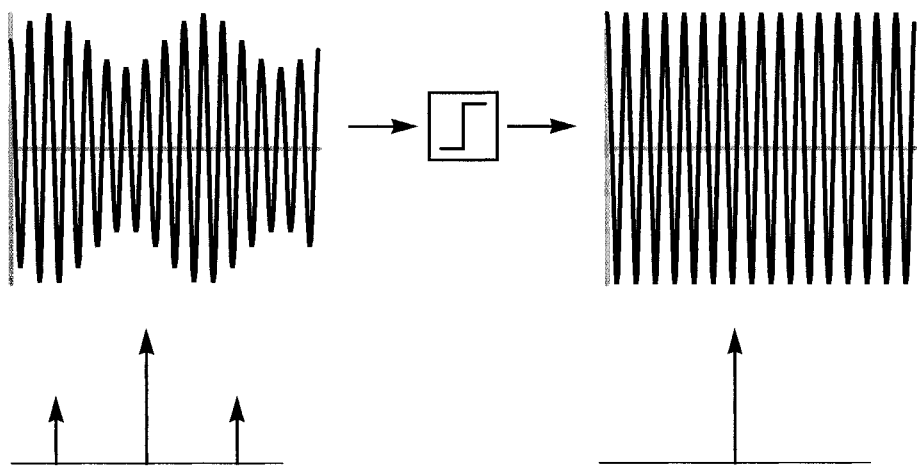


FIGURE 6 Limiter removes AM sidebands leaving only the carrier.



power of the fundamental. If the oscillation waveform is defined by (1) then phase noise is given by:

$$\mathcal{L}(f_m) = \frac{S_v(f_m)}{A^2/2} \quad (10)$$

where  $S_v(f_m)$  is the power spectral density of the oscillation signal  $v(t)$ .

In other words, phase noise is the noise to carrier ratio. Note that this definition does not exclude amplitude perturbations. However, in an oscillator, amplitude noise is naturally rejected by the limiting action inherent in any real implementation.

Graphically, phase noise can be explained as in Figure 7 depicting the output spectrum of an oscillator. When the oscillator is noise-free, its power spectrum is a delta Dirac impulse. An oscillation that is modulated with white noise is known to have the shape of a Lorentzian pulse (the power gain of a first order lowpass filter) [4]. While the total power in the modulated oscillation remains the same for the noisy and the noise-free oscillation, the broadening of the output spectrum is a characteristic of autonomous oscillators. The noise power around the average oscillator frequency is also known as the phase noise skirt. In any non-autonomous (driven) linear or nonlinear circuit, if the input to the circuit is a single tone, the output is an overlay of a single tone and noise. That is to say the output spectrum can be decomposed into a delta-Dirac impulse and a background noise. In oscillators, since the system lacks an external time reference, the output spectrum is not a delta-Dirac impulse except in the noiseless case [6]. Instead, the output spectrum is that of a Lorentzian pulse. This is known as linewidth broadening by analogy with lasers, which are optical oscillators.

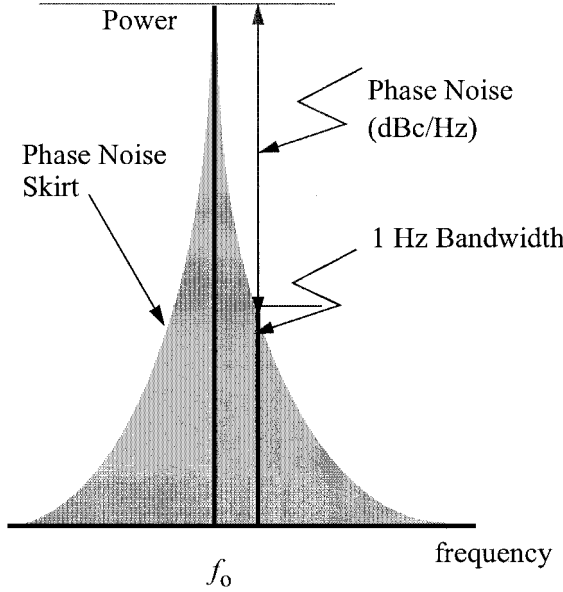
To evaluate phase noise numerically using (10), it is first necessary to evaluate the power spectral density of the output voltage. There are a myriad of ways to evaluate this for a generic oscillator. One approach was given by Edson [9,10] and later by Herzel [4] and is summarized below.

The starting point is the oscillation voltage waveform given by (1). The instantaneous frequency noise is given by

$$f_n(t) = \frac{d}{dt}\phi_n \quad (11)$$

Phase noise is described by Wiener process and the power spectral density of phase noise is characterized by its  $-20$  dB/dec slope. Therefore the *frequency*

FIGURE 7 Phase noise skirt.



noise spectrum has to be flat [4]. Implicitly, this assumes that the frequency perturbation is a linear function of the noise voltage causing it.

With the assumption that  $f_n$  has a white spectrum, the autocorrelation function of  $f_n$  is given by

$$R_{f_n}(\tau) = 2D\delta(\tau) \quad (12)$$

Next we look into the autocorrelation function of  $v(t)$  as follows

$$R_v(\tau) = E\langle (v(t+\tau))(v(t)) \rangle \quad (13)$$

Substituting with (1) into (13), and using basic trigonometry, the following can be readily shown

$$R_v(\tau) = \frac{A^2}{2} ([\cos(\omega_0 t)E(\cos(\phi(t+\tau) - \phi(t)))] - [\sin(\omega_0 t)E(\sin(\phi(t+\tau) - \phi(t)))] \quad (14)$$

The quantity given by  $\phi(t + \tau) - \phi(t)$  is a random variable with a symmetric distribution, which makes the expected value of  $\sin(\phi(t + \tau) - \phi(t))$  equal to zero. With this in mind, (14) reduces to:

$$R_v(\tau) = \frac{A^2}{2} ([\cos(\omega_o t) E(\cos(\phi(t + \tau) - \phi(t)))] \quad (15)$$

Taking the Fourier transform of (15), we arrive at the power spectral density of  $v(t)$ :

$$S_v(\omega) = A^2 \frac{D}{(\omega - \omega_o)^2 + D^2} \quad (16)$$

This shows how the power spectrum of an oscillator takes the shape of a Lorentzian pulse if only white noise is considered. It is clear that the spectrum at zero frequency does not explode to infinity as could happen in a mixer driven by a perfect sinewave.

Substituting in (10), oscillator's phase noise is given by:

$$\mathcal{L}(\omega - \omega_o) = \frac{2D}{(\omega - \omega_o)^2 + D^2} \quad (17)$$

For a reasonable quality oscillator, the diffusivity  $D$  is a small quantity, meaning that phase diffusion process is slow. Intuitively, this means that the initially synchronized oscillators discussed earlier will take a long time to lose coherence. For frequency offsets  $\Delta\omega = \omega - \omega_o \gg D$ , phase noise is given by:

$$\mathcal{L}(\Delta\omega) \approx \frac{2D}{\delta\omega^2} \quad (18)$$

This explains the statement that phase noise at white-noise-dominated offset has a slope of  $-20$  dB/decade. Note again that colored noise is not considered here at all.

It should be clear that  $D$  establishes the relationship between phase noise and timing jitter in an oscillator. It should also be noted that we assume that the relationship between the continuous phase modulation  $\phi$  and the discrete-time phase error  $\theta$  is given by [3]:

$$S_{\theta}(\omega) = S_{\phi}(\omega) \quad (19)$$

To find an expression for  $D$ , first re-write (7) as follows:

$$\sigma_{\theta}^2 = 2DT \quad (20)$$

For the  $n^{\text{th}}$  oscillation period, the discrete phase error  $\theta_n$  is given by:

$$\theta_n = \omega_o(T_n - 2\pi) = \frac{2\pi}{T}(T_n - T) \quad (21)$$

Accordingly, the period jitter is given by:

$$\sigma_j^2 = \left(\frac{T}{2\pi}\right)^2 \sigma_{\theta}^2 \quad (22)$$

Finally, we arrive at an expression for  $D$  using (20) and (22)

$$\sigma_j^2 = D \frac{T^3}{8\pi^2} \quad (23)$$

Substituting from (23) into (17) or (18) establishes the relationship between jitter and phase noise for an oscillator with only white noise sources. Without much effort, it is trivial to show that

$$\sigma_j = \sqrt{\frac{\mathcal{L}(\Delta\omega)\Delta\omega^2}{\omega_o^3}} \quad (24)$$

---

## 6 Oscillator Phase Noise Models: Post-Leeson

The past few years have witnessed an explosion in oscillator phase noise research. Various models for the phenomena are built and evaluated. In addition, multiple simulators are available in the mass market to accurately predict the phase noise performance of the oscillator. The models available are very rigorous. The intuition and design guidelines are not always clear. In this section, we discuss what we consider the most important models in recent years and show briefly the key idea of the model we build and advocate in this book. We will limit the discussion to key ideas without delving into the math-

emational details. We will show briefly the strengths and weaknesses of each model.

### **6.1 Hajimiri's Model**

The model was originally presented in [8] as a general theory for phase noise in electrical oscillators. It averts the nonlinear analysis by treating the oscillator as a linear but time-varying system. The model further assumes that noise in an oscillator is a cyclostationary random process. Cyclostationarity means that the first and second-order statistics of the random process are periodic with a period  $T$ . Where  $T$  in an oscillator is the period of oscillation. Therefore, the oscillator is called a  $T$ -periodic system in that the oscillation waveform repeats itself every  $T$  seconds. The model builds on the following assumptions:

1. white noise can be treated as uncorrelated random samples in time (impulses)
2. the response of the oscillator to a noise sample depends on the time that sample occurs with respect to the oscillation waveform such that:
  - a. noise that occurs at the peak of oscillation can only create amplitude noise.
  - b. noise that occurs at the zero-crossings of oscillation can only create phase noise.

Based on these assumptions, Hajimiri develops what is called an Impulse Sensitivity Function (ISF). It measures the sensitivity of the phase of the oscillator to a small perturbation current injected at a particular moment in time. The ISF has the same period  $T$  of the oscillator itself because of the cyclostationarity assumption. A simulation procedure was also presented in [8], by which means, the ISF can be constructed. Using a SPICE-like transient simulator, the ISF can be evaluated from each noise source in the oscillator to the output. An impulse of current, representing noise in a transistor channel or a resistor etc., is injected into the oscillator at one instant in time. The effect on the oscillator phase is evaluated after multiple cycles when the oscillator is back to its normal limit cycle. The position of the impulse is shifted with respect to the oscillation waveform and simulation is re-run to evaluate the ISF from a particular noise source at a different time point. Using a fairly tedious simulation procedure, the ISF of each noise source is constructed.

To graphically explain the model, consider the waveforms of an oscillation with an injected noise current into the tank. Injecting an impulse current into the tank while the waveform is at the peak, changes only the amplitude of oscillation as shown in Figure 8a. This change in amplitude is rejected by the oscillator due to the presence of the intrinsic nonlinearity of the oscillator and the oscillator manages to restore its original amplitude after a few cycles<sup>†</sup>. Alternatively, if the noise is injected at the zero crossing, only the phase of the oscillation changes as shown in Figure 8b. Phase disturbance does not fade away because the oscillator has no particular phase preference. The accumulated phase jitter is given by the integral:

$$\phi(t) = \frac{1}{q_{\max}} \int_{-\infty}^t \Gamma(\omega_o \tau) i_n(\tau) d\tau \quad (25)$$

where  $q_{\max}$  is the maximum charge on the tank capacitance and  $\tau$  is the time instant at which noise was injected.  $\Gamma$  is the ISF from the noise current source,  $i_n(\tau)$ , to the oscillator's phase.

The model assumes linear operation but accounts for time variance. This allows the extension of the model to multiple noise sources once correlation between these sources is accounted for. To account for the time variance of noise in various circuit elements, the noise current is decomposed into a white noise part and a time scaling function as follows:

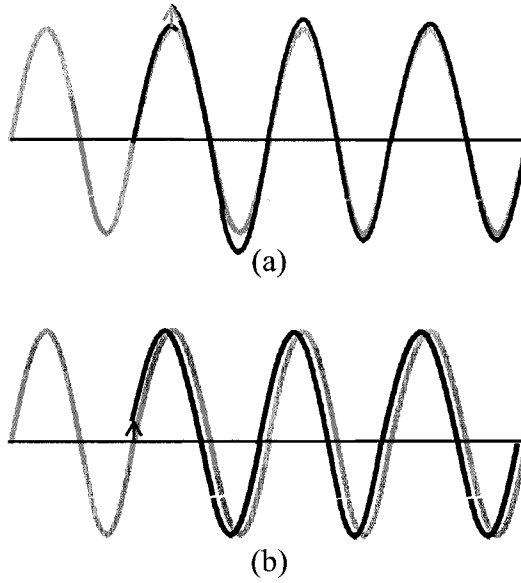
$$i_n(\tau) = i_{no}(\tau) \alpha(\omega_o t) \quad (26)$$

With the cyclostationarity assumption,  $\alpha$  is a  $T$ -periodic function.

It is always instructive to consider the oscillator in the state-space plane. An LC oscillator is a second order system, i.e. it possesses two states: capacitor voltage and inductor current. Plotting the inductor current versus the capacitor voltage shows a closed curve (in signal processing terminology it is called a limit cycle). As the voltage across the capacitor changes, so does the inductor current such that the locus repeats every  $T$  seconds. However, the oscillator does not necessarily traverse the locus at constant rotational speed. The forgo-

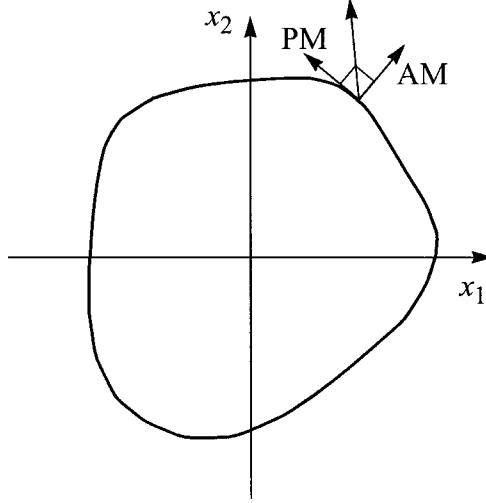
<sup>†</sup> In an ideal lossless LC tank, the amplitude of oscillation never returns to its original value after a noise impulse. This is because there is no dissipative loss to change the total energy of the tank nor there is nonlinearity to fix the amplitude of oscillation.



FIGURE 8 *Impulse response of an oscillator using Hajimiri's model.*

ing assumptions of the model can be explained in the state-space plane shown in Figure 9. Any perturbation can be decomposed into a tangential component to the state-space locus and one perpendicular to it. According to this linear time-varying model, the tangential component disturbs only the oscillator's phase whereas the perpendicular component is pure amplitude noise. Later we will discuss another form of perturbation decomposition.

The model gave some insight into the operation of oscillators. One of its advantages is that it is applicable to any class of oscillators, not only LC or ring-based ones. It provides a simulation procedure that shows reasonable accuracy using a SPICE-like transient simulator and was published at a time where simulators like SpectreRF and EldoRF were not very common. However, it does not formally address flicker noise at all. The treatment of flicker noise in the original paper [8] is performed in the frequency domain rather than the time domain without clear analysis or conclusive answers. The model found wide acceptance at least for its thermal noise treatment. Later, it was deemed accurate only for cases where injected noise is stationary. As a result, the model cannot be used for quadrature oscillators for example [11]. As we

FIGURE 9 *Orthogonal decomposition of perturbation.*

will see in the discussion of Demir's model, the assumption of cyclostationarity leads to an output spectrum that rises to infinity at the oscillation frequency [12]. Therefore, the output spectrum under Hajimiri's model does not resemble a Lorentzian pulse. This particular inaccuracy does not impact the overall accuracy of the model because for a reasonable quality oscillator, the Lorentzian pulse shape dies out quickly as given by (18).

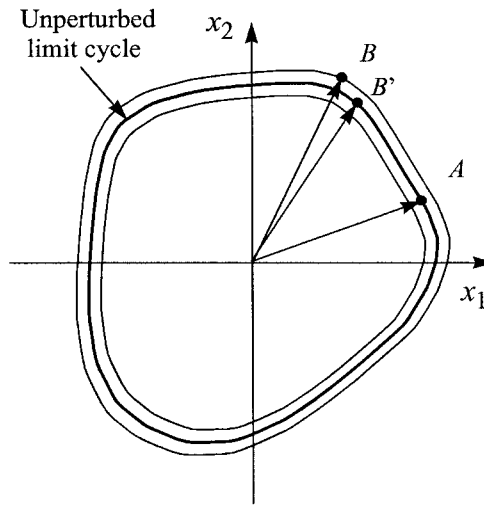
In essence, the model was developed as a simulation methodology. The circuit intuition is gleaned through extensive simulations rather than analytical means. Therefore, there is no systematic way to understand the physics of why a particular topology behaves in a particular way, or what happens if the device width is changed. Despite following efforts to draw more insights, the intuition remains based on extensive simulations and clever observation rather than circuit analysis or physical insight [5].

## 6.2 Demir's Model

Unlike Hajimiri's model, this work by Demir does not assume cyclostationarity. In fact, the model shows that the oscillator output voltage is a stationary random process. This is justified by the fact that the oscillator has no external time base to set a cyclostationarity period. The model adopts a nonlinear per-

turbation analysis whereby the perturbation is not decomposed into phase and amplitude noise components. Instead, the perturbation is decomposed into a phase deviation component and an additive component that Demir calls orbital deviation. To illustrate the basic concepts, let's resort to the state-space plane. Consider the oscillator without noise with a limit cycle traversing a certain orbit as shown in Figure 10. When noise sources are considered, the oscillator does not follow the original orbit but can have any orbit within a particular band of orbits. The model encompasses the decomposition of the perturbation into two components:

FIGURE 10 *Kartner's decomposition.*



1. Phase deviation component responsible for shifting the phase of the oscillator.
2. Orbital deviation, by which means, the oscillator's limit cycle is momentarily perturbed.

This decomposition was first proposed by Kartner [13]. Demir distinguishes between the two components of perturbation in the following manner: the orbital deviation does not accumulate and its impact on the oscillator's limit cycle dies to zero if the perturbation is removed. Phase deviation, on the other hand, accumulates and if the perturbation source is removed the phase error

produced during the time of perturbation remains indefinitely. Consider the state-space plot in Figure 10. At a particular point in time, the oscillator was at point  $A$  on the unperturbed locus. If noise is included, the accumulation of phase error can result in the oscillator's state being at point  $B$  instead. Clearly, point  $B$  is not close to point  $A$  as the phase error can grow without bound. Point  $B$  however, can be projected on another point  $B'$  that falls on the unperturbed limit cycle as well as a small component for  $B'$  to  $B$ . The translation of the oscillator's phase from  $A$  to  $B'$  is caused by the phase deviation component. The component from  $B'$  to  $B$  is the orbital deviation. Using a relatively complicated mathematical description, entailing stochastic differential equations, Demir manages to find a proper and formal description of the output spectrum of the VCO in the presence of thermal noise. Of most significance, is the proof that the oscillator output is not cyclostationary but rather a stationary process. The phase of the oscillator is non stationary, as would be expected of an integrated noise. Demir's argument for the physical origin of stationarity in the output voltage of the oscillator is also interesting. He recognizes that the oscillator's period is disturbed by noise, which means that it cannot set a proper cycle for a cyclostationary random process. Using the original terminology, the oscillator is represented by a group of equations in the form:

$$\frac{\partial}{\partial t}x(t) = f(x(t)) \quad (27)$$

where  $x(t)$  is the oscillator's output voltage.

When the oscillator is perturbed by a small perturbation  $b(t)$ , the output voltage takes the form  $x(t + \theta(t)) + y(t)$ , where  $y(t)$  is the orbital deviation.

The phase noise resulting from the voltage perturbation  $b(t)$  can be obtained by solving the following equation:

$$\frac{\partial \theta}{\partial t} = v(t + \theta(t))B(t + \theta(t))(b(t)) \quad (28)$$

where  $v$  is called the perturbation projection vector and plays a similar role to the ISF in Hajimiri's analysis and  $B$  captures the response of the system of equations in (27) to the perturbation  $b$ .

The proposed solution is acquired using a nonlinear two-step perturbation analysis. Using the perturbation proposed by Kartner, the equation system given by (27) is first solved by assuming no orbital deviation to yield a solution that has only the accumulated phase error. Later, the resulting solution is re-solved including a small perturbation using linear perturbation.

As shown by other researchers, Demir shows that the spectrum of an oscillator is a Lorentzian pulse in the presence of white noise. Demir further extended his modeling to include colored noise source, which Hajimiri's model does not cover. He first redefines the flicker noise spectrum as that which causes 0 dBc at zero frequency in an oscillator and solves a system of stochastic differential equations to find the output spectrum of an oscillator in the presence of colored noise [14].

In a recent publication, a comparison between Demir's work on white noise and that of Hajimiri was drawn [11]. It shows that the two models are identical in the case of stationary noise. It also shows that in the case of quadrature oscillators Hajimiri's equations collapse whereas those of Demir still yield the correct result. Again, Demir's work is valid for all classes of oscillators. No independent verification of Demir's flicker noise work is available to date.

Demir's model is perhaps the most generic and most accurate treatment of noise in oscillators. It is mathematically involved and perfectly suited for a simulator-type application. It does not help circuit designers know how to design the best oscillator or how to improve on existing topologies by showing the mechanisms of phase noise generation. There is almost no intuition into circuits that results from Demir's model but it is definitely a remarkable addition to the simulation of phase noise in oscillators.

## **6.3 A Mechanistic Physical Model for LC Oscillators**

### **6.3.1 Yet Another Model!**

The work presented here can be what is expected from a circuit designer analyzing oscillators. The basic assumptions are closer to those of Hajimiri. We assume a  $T$ -periodic system disturbed by cyclostationary noise. This cyclostationarity does not appear explicitly in the model equations but it is nevertheless implicit. The model assumes a steady-state solution to the circuit<sup>†</sup>, by which means, a large signal sinusoid exists across the tank and random noise sources from circuit elements disturb the amplitude and phase of the oscilla-

tor. Unlike Demir and Hajimiri, the work presented here is focused on LC oscillators. Even though the circuit analysis can perhaps be extended to other classes of oscillators, this book does not cover any other than LC oscillators. In essence, the model is built by circuit designers and is intended to be used also by circuit designers.

The model is valid, nevertheless, for both single phase and quadrature oscillators as we will show in the following chapters. Our model handles flicker noise in a systematic way, unlike the linear time-invariant model presented earlier. The model results in closed form expressions rather than a numerical procedure. Therefore, it is best suited for circuit designers who are interested in designing real-life circuits.

### 6.3.2 Basics of the Approach

Noise from any source in the oscillatory system can be represented by a number of sinusoids evenly distributed every 1 Hz. These are called conformal signals [16]. If the oscillator is disturbed by a small tone at a particular offset with any random phase, the FFT of the oscillator output can tell what happens to both the amplitude and phase of the injected tone. Due to the large signal operation of the circuit, the gain seen by the injected noise sinusoid can possibly entail frequency translation [15]. Therefore, we call this gain the translation gain. Determining translation gain is possible using transient simulation and an FFT step. It can be also determined using a periodic steady state simulator like SpectreRF. Translation gain has to take noise folding into account. Noise folding occurs because thermal noise has an infinite bandwidth. As a result, noise is under-sampled by both the fundamental tone and the harmonics of the oscillation. Aliases of the under-sampled noise fold to near the fundamental frequency. As shown in Chapter 1 and also in [16], a single-sideband injected into the tank can be decomposed into four components of correlated phases such that it represents both amplitude and phase modulation. The phase information of the FFT can easily show AM and PM sidebands to any degree of accuracy required.

The work presented however, does not resort to simulations to determine the translation gains from each noise source to the output. Instead, we resort to circuit analysis to determine the AM and PM components.

---

† This is also the underlying assumption in a simulator like SpectreRF

We begin by assuming a steady-state solution, in which there exists the oscillator tone and four sideband modulation tones representing AM and PM. Of course we assume one single source of noise in the oscillator at a time. Each sideband is scaled by an unknown coefficient that needs to be determined using circuit equations in steady state. Once the coefficients are determined, the type of noise (AM or PM) resulting from that noise source is known. The analysis is done for all noise sources. The circuit equations used take into consideration the physical mechanism behind any frequency translations or scaling. More details on the technique will be shown in the following chapter.

Dealing with noise sources in frequency domain rather than time domain has its advantages. The most important one is that it facilitates the analysis of colored noise sources. For example, flicker noise at any frequency is uncorrelated with flicker noise at any other frequency. This greatly simplifies the analysis. However, as we will show, normal frequency translations of flicker noise can only result in amplitude noise. We will also show that flicker noise can create phase noise in the oscillator by means of frequency modulation processes.

The collective analysis presented in the following chapters is what we call a physically-based mechanistic model. It is physical because it relates to actual operation of the circuit elements. It is mechanistic as it describes the behavior of the oscillator using a group of mechanisms rather than a unified numerical methodology. This allows the full optimization of the oscillator by understanding the mechanisms in action that are responsible for phase noise generation. The model is very intuitive while resulting in a reasonable accuracy, within 1 dB of what SpectreRF predicts.

---

## **References**

- [1] David D. Allan, Neil Ashby, and Clifford C. Hodge, "The science of timekeeping," Hewlett-Packard, Application Note 1289, 1997.
- [2] John A. McNeil, "Jitter in ring oscillators," *IEEE J. of Solid-State Circuits*, vol. 32, no. 6, June 1997.
- [3] David C. Lee, "Analysis of jitter in phase-locked loops," *IEEE Trans. on Circuits and Systems-II Analog and Digital Signal Processing*, vol. 49, no. 11, Nov. 2002.

- [4] F. Herzel and B. Razavi, "A study of oscillator jitter due to supply and substrate noise," *IEEE Trans. on Circuits and Systems-II: Analog and Digital Signal Processing*, vol. 46, no. 1, pp. 56-62, Jan. 1999.
- [5] D. Ham, and A. Hajimiri, "Virtual damping and Einstein relation in oscillators", *IEEE J. of Solid-State Circuits*, vol. 38, no. 3, pp. 407-418, Mar. 2003.
- [6] M. Lax, "Classical noise V. Noise in self-sustained oscillators," *Phys. Rev.*, CAS-160, no. 2, pp. 290-307, Aug. 1967.
- [7] F. Herzel, "An analytical model for the power spectral density of a voltage-controlled oscillator and its analogy to the laser linewidth theory," *IEEE Trans. on CAS-I: Fund. Theory and Tech.*, vol. 45, no. 9, pp. 904-908, Sep. 1999.
- [8] A. Hajimiri, and T. H. Lee, "A general theory of phase noise in electrical oscillators," *IEEE J. of Solid-State Circuits*, vol. 33, no. 2, pp. 179-194, Feb. 1997.
- [9] W. A. Edson, "Noise in oscillators," *Proc. IRE*, pp.1454-1466, Aug. 1960.
- [10] Ali Hajimiri, and Thomas H. Lee, *The Design of Low Noise Oscillators*, Kluwer Academic Publishers, 1999.
- [11] P. Vanassche, G. Gielen, and W. Sansen, "On the difference between two widely publicized methods for analyzing oscillator phase behavior," in *Proc. of Int. Conf. on Computer-Aided Design, ICCAD*, 2002.
- [12] A. Demir, A. Mehrorta, and J. Roychowdhury, "Phase noise in oscillators: a unifying theory and numerical methods for characterization," *IEEE Trans. on Circuits and Systems-I Fundamental Theory and Applications*, vol. 47, no. 5, pp. 655-674, May 2000.
- [13] F. K. Kartner, "Analysis of white and  $f^{-1}$  noise in oscillators," *Int. J. Circuit Theory Appl.*, vol. 18, pp. 489-519, 1990.
- [14] A. Demir, "Phase noise and timing jitter in oscillators with colored-noise sources," *IEEE Trans. Circuits and Systems-I: Fundamental Theory Appl.* vol. 48, no. 12, pp. 1782-1791, Dec. 2002.
- [15] Joel Phillips and Ken Kundert, "Noise in mixers, oscillators, samplers, and logic: an introduction to cyclostationary noise," [www.designers-guide.com/Theory](http://www.designers-guide.com/Theory).
- [16] W. A. Robins, *Phase Noise in Signal Sources*, IEE Press, 1982.



The Designer's Guide to High-Purity Oscillators

Hegazi, E.E.; Rael, J.; Abidi, A.

2005, XII, 204 p., Hardcover

ISBN: 978-1-4020-7666-4